

# Artificial Light-harvesting Antenna Systems Grafted on a Carbohydrate Platform

**Paola Bonaccorsi,<sup>\*a</sup> Maria Chiara Aversa,<sup>a</sup> Anna Barattucci,<sup>a</sup> Teresa Papalia,<sup>b</sup> Fausto Puntoriero<sup>\*a</sup> and Sebastiano Campagna<sup>\*a</sup>**

<sup>a</sup> *Dipartimento di Scienze Chimiche, Università di Messina, viale F. Stagno d'Alcontres 31, Messina, Italia.*

<sup>b</sup> *Dipartimento di Scienze del farmaco e dei prodotti per la salute, Università di Messina, villaggio SS. Annunziata, Messina, Italia.*

## SUPPORTING INFORMATION

### Table of Content

General experimental methods.....	S1-S2
Calculation of energy transfer rate constants.....	S2
Estimation of the efficiency of energy transfer.....	S2
Calculation of the overlap integral for Förster energy transfer in <b>1</b> and <b>2</b> .....	S3-S4
Detailed procedure for the synthesis of compound <b>6</b> .....	S5
Detailed procedure for the synthesis of compound <b>1</b> .....	S6
Detailed procedure for the synthesis of compound <b>7</b> .....	S7
Detailed procedure for the synthesis of compound <b>2</b> .....	S8
Absorption and luminescence spectra of <b>6</b> and <b>7</b> .....	S9-S10
Calculated sum spectra of <b>6</b> (one- or three-fold) plus <b>7</b> versus absorption spectra of <b>1</b> and <b>2</b> .....	S11
Excitation spectra of <b>1</b> and <b>2</b> .....	S12-S13
Emission spectra of mixtures (1:1 and 3:1 molar ratio) of <b>6</b> and <b>7</b> in comparison with emission spectra of <b>1</b> and <b>2</b> (excitation wavelength 360 nm).....	S14
Transient absorption spectra of <b>6</b> and <b>7</b> .....	S15-S17
References.....	S18
<sup>1</sup> H and <sup>13</sup> C NMR spectra for <b>1</b> , <b>2</b> , <b>6</b> and <b>7</b> and COSY for <b>3</b> , <b>6</b> and <b>7</b> .....	S19-S29

## General experimental Methods

### Synthesis

Solvents were purified according to standard procedures. All reactions were monitored by TLC on commercially available precoated plates (Aldrich silica gel 60 F254) eluted with Hexane/EtOAc, or Hexane/EtOAc/DCM, and the products were visualized with vanillin [1 g dissolved in MeOH (60 mL) and conc. H<sub>2</sub>SO<sub>4</sub> (0.6 mL)]. Silica gel used for column chromatography was Aldrich 60. <sup>1</sup>H and <sup>13</sup>C NMR spectra were recorded in acetone-*d*<sub>6</sub> with a Varian Mercury 300 spectrometer at 300 and 75 MHz, and with a Varian 500 spectrometer at 500 and 125 MHz, respectively; the attributions are supported by Attached Proton Test (APT) and Heteronuclear Single Quantum Coherence (HSQC) experiments and Correlation spectroscopy (COSY).

### Equipment and methods for the absorption spectroscopy and photophysical experiments

UV/Vis absorption spectra were taken on a Jasco V-560 spectrophotometer. For steady-state luminescence measurements, a Jobin Yvon-Spex Fluoromax 2 spectrofluorimeter was used, equipped with a Hamamatsu R3896 photomultiplier. The spectra were corrected for photomultiplier response using a program purchased with the fluorimeter. For the luminescence lifetimes, an Edinburgh OB 900 time-correlated single-photon-counting spectrometer was used. As excitation sources, a Hamamatsu PLP 2 laser diode (59 ps pulse width at 408 nm) and/or the nitrogen discharge (pulse width 2 ns at 337 nm) were employed. Emission quantum yields for deaerated solutions were determined using the optically diluted method.<sup>1</sup> As luminescence quantum yield standards, we used [Ru(bpy)<sub>3</sub>]<sup>2+</sup> (bpy = 2,2'-bipyridine),<sup>2</sup> cresyl violet<sup>3</sup> and tetramethoxy-bisindolodipyrromethene-difluoroborate.<sup>4</sup>

Time-resolved transient absorption experiments were performed using a pump-probe setup based on the Spectra-Physics MAI-TAI Ti:sapphire system as the laser source and the Ultrafast Systems Helios spectrometer as the detector. The output of laser beam was split to generate pump and probe beam pulses with a beam splitter (85 and 15%). The pump pulse (400 nm, 1-2 μJ) was generated with a Spectra-Physics 800 FP OPA and was focused onto the sample cuvette. The probe beam was delayed with a computer controlled motion controller and then focused into a 2-mm sapphire plate to generate a white light continuum (spectral range 450–800 nm). The white light is then overlapped with the pump beam in a 2-mm quartz cuvette containing the sample. The effective time resolution was ca. 200 fs, and the temporal chirp over the white-light 450–750 nm range ca. 150 fs; the temporal window of the optical delay stage was 0–3200 ps. Please note that all the transient spectra shown in the present paper are chirp corrected. The chirp correction was done by using the pump induced absorption signals themselves in the same conditions (same cuvette, solvent, temperature,

stirring frequency...) used for each single experiment. The time-resolved data were analyzed with the Ultrafast Systems Surface Explorer Pro software. Experimental uncertainties on the absorption and photophysical data are as follows: absorption maxima, 2 nm; molar absorption, 15%; luminescence maxima, 4 nm; luminescence lifetimes, 10%; luminescence quantum yields, 20%; transient absorption decay and rise rates, 10%.

### Calculation of energy transfer rate constants

The energy transfer rate constants reported in the text are based on the transient absorption spectroscopy data, and have been obtained by comparing the time constants for the recovery of the 500 nm bleach in **1** and **2** (250 fs and 12 ps, respectively) with the time constant (longer than 2 ns) exhibited for the recovery of the corresponding bleach in **6**, which contains only an **A**-type chromophore, using the usual equation 1.

$$k_{\text{et}} = (1/\tau') - (1/\tau^0) \quad (1)$$

In eq. (1),  $k_{\text{et}}$  is the calculated energy transfer rate constant and  $\tau'$  and  $\tau^0$  are the lifetimes of the quenched (the 500 nm bleaching recovery time constant of **1** and **2**) and unquenched (the 500 nm bleaching recovery of **6**) lifetimes of the **A**-based excited states, respectively. In the specific case, since  $(2 \text{ ns})^{-1}$  is neglectable compared to  $(250 \text{ fs})^{-1}$  and  $(12 \text{ ps})^{-1}$ , the rate constants for energy transfer from the excited state of **A**-based subunit(s) to the excited state of **B**-based subunit in **1** and **2** have been approximated to these latter values, respectively, that is  $4 \times 10^{12} \text{ s}^{-1}$  and  $8 \times 10^{10} \text{ s}^{-1}$ .

### Estimation of the efficiency of energy transfer in **1** and **2**

Since detection of emission of the higher-energy BODIPY subunit in **1** and **2** is below the limit of our equipment, the estimation of the efficiency of energy transfer,  $\eta(\text{ET})$ , in **1** and **2** (like the calculation of the energy transfer rate constants) is based on transient absorption spectroscopy data. The percentage of the energy transfer efficiency is therefore estimated by equation 2.

$$\eta(\text{ET}) = (\tau')^{-1} / [(\tau^0)^{-1} + (\tau')^{-1}] \times 100 \quad (2)$$

In eq. (2),  $\tau'$  and  $\tau^0$  have the same meanings reported above. For both **1** and **2**, energy transfer efficiency is >99%.

### Calculation of the overlap integral between donor emission and acceptor absorption spectra for energy transfer processes in **1** and **2**

The overlap integral  $J$  for Förster interaction was calculated according to equation 3.

$$J_F = \frac{\int F(\bar{\nu})\epsilon(\bar{\nu})/\bar{\nu}^4 d\bar{\nu}}{\int F(\bar{\nu})d\bar{\nu}} \quad (3)$$

In this equation,  $F(\bar{\nu})$  is the luminescence spectrum of the donor (compound **6**), and  $\epsilon(\bar{\nu})$  is the absorption spectrum of the acceptor (compound **7**), on an energy scale ( $\text{cm}^{-1}$ ).

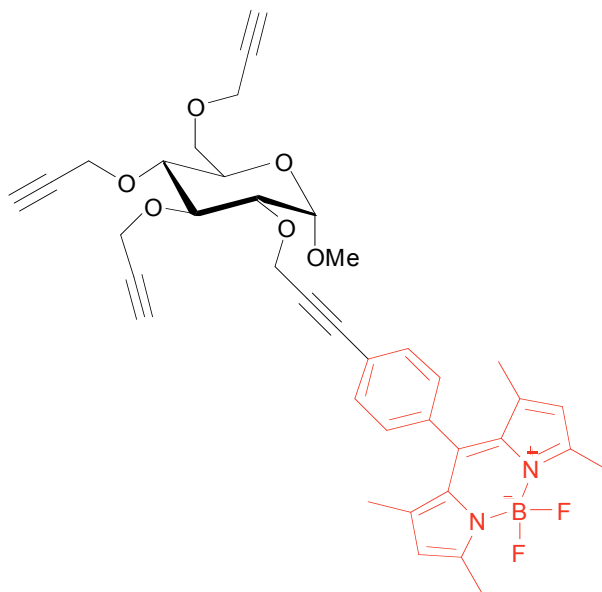
The calculated  $J$  value is compatible with ultrafast energy transfer rate constant for very short donor-acceptor distances (as in **1**) and relatively fast rate constant at slightly longer distances (as for some partners in **2**), when the usual, simplified Förster equation (4) is used.<sup>5</sup>

$$k_{en}^F = 8.8 \times 10^{-25} \frac{K^2 \Phi}{n^4 r_{AB}^6 \tau} J_F \quad (4)$$

In eq. 4,  $k_{en}^F$  is the rate constant of the energy transfer process,  $K$  is an orientation factor which accounts for the directional nature of the dipole-dipole interaction,  $\Phi$  and  $\tau$  are the luminescence quantum yield and lifetime of the donor, respectively,  $n$  is the solvent refractive index,  $r_{AB}$  is the distance (in Å) between donor and acceptor. Since each bodipy subunit is freely rotating along the triple bond axis, the random value for the orientation factor (0.667) is assumed. In particular, using the calculated  $J$  value ( $1.42 \times 10^{-13} \text{ cm}^6$ ) for **1** and **2**, the relevant parameters derived from the absorption spectrum of **7** (model for the acceptor unit in **1** and **2**) and the luminescence properties of **6** (model for the donor units in **1** and **2**), and assuming 10 Å as donor-acceptor distance in **1**, an energy transfer rate constant of 200 fs is calculated for this species, in impressive agreement with the experimental results. For **2** assuming an averaged donor-acceptor distance related to the two more distant BODIPY donors and the acceptor one of 19.5 Å, rate constant for the Foerster energy transfer process is 13 ps, also in impressive agreement with the experimental results (12 ps). Donor-acceptor distances (center-to-center) have been calculated using computer-optimized structures.

**Methyl-2,3,4,6-tetra-*O*-propargyl- $\alpha$ -D-glucopyranoside (3).** It was synthesized following literature procedures.<sup>6</sup> <sup>1</sup>H NMR:  $\delta$  4.85 (d, <sup>3</sup>*J* = 3.4 Hz, 1H), 4.48-4.40 (m, 4H), 4.33 (d, <sup>4</sup>*J* = 2.4 Hz, 2H), 4.22 (d, <sup>4</sup>*J* = 2.0 Hz, 2H), 3.81 (dd, <sup>4</sup>*J* = 1.5 Hz, <sup>2</sup>*J* = 10.7 Hz, 1H), 3.76 (t, <sup>3</sup>*J* = 9.3 Hz, 1H), 3.68 (dd, <sup>3</sup>*J* = 5.3 Hz, *J* = 10.7 Hz, 1H), 3.61 (m, 1H), 3.51 (dd, *J* = 3.4 Hz, *J* = 9.8 Hz, 1H), 3.40 (dd, *J* = 8.8 Hz, *J* = 9.8 Hz, 1H), 3.36 (s, 3H), 2.99-2.92 (m, 4H).

### Compound 6.

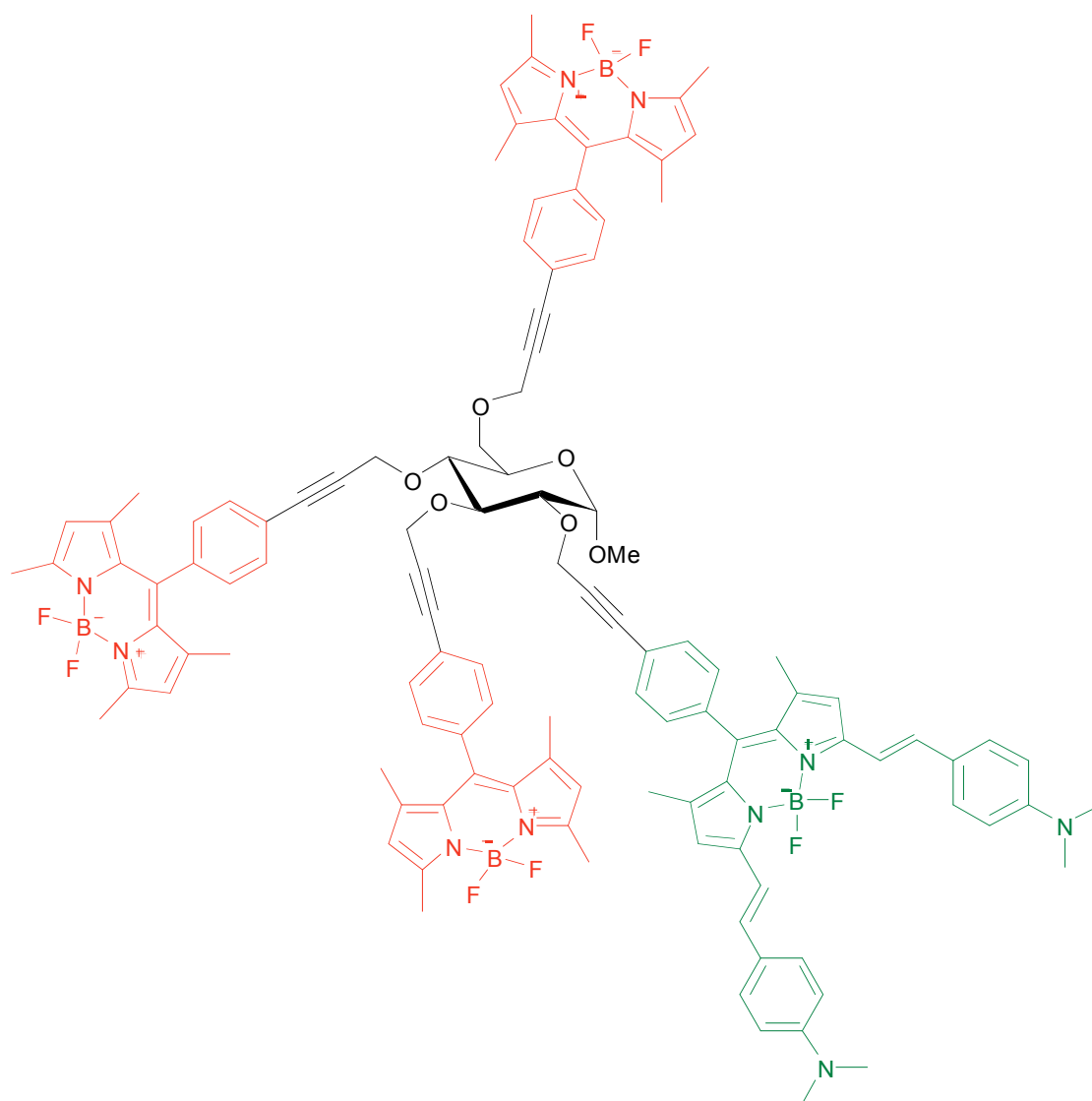


[Pd(PPh<sub>3</sub>)<sub>4</sub>] (0.11 mmol) was added to a degassed solution of boron difluoro-2-[(3,5-dimethyl-2*H*-pyrrole-2-ylidene)-(4-iodophenyl)methyl]-3,5-dimethyl-1*H*-pyrrolate (**4**) (500 mg, 1.11 mmol) and methyl-2,3,4,6-tetra-*O*-propargyl- $\alpha$ -D-glucopyranoside (**3**) (2.65g, 8.88 mmol) in DMF/Triethylamine (TEA) (28 ml, 1:1). The mixture was heated, at 60°C, under argon, for 3 h, until the disappearance of compound **4** was observed by TLC (Hexane /EtOAc 7:3). Solvents were removed under reduced pressure. The reaction crude was subjected to gel-filtration on silica, eluting with Hexane/Ethyl acetate (70:30), and to silica gel column chromatography, using DCM/Hexane/EtOAc (70:25:5) as eluants, for obtaining compound **6** as an orange low melting solid (0.28 g, 0.44 mmol, 40 %). TLC: *R<sub>f</sub>* 0.55 (eluant DCM/Hexane/EtOAc 7:2.5:0.5). <sup>1</sup>H NMR:  $\delta$  7.71 (d, *J* = 8.3 Hz, 2H), 7.44 (d, *J* = 8.3 Hz, 2H), 6.12 (s, 2H), 4.96 (d, *J* = 3.4 Hz, 1H), 4.63 and 4.60 (AB system, *J* = 16.5 Hz, 2H), 4.52-4.43 (m, 4H), 4.22 (d, *J* = 2.4 Hz, 2H), 3.83-3.79 (m, 2H), 3.69 (dd, *J* = 4.9, *J* = 10.8 Hz, 1H), 3.66-3.60 (m, 2H), 3.44 (dd, *J* = 8.8 *J* = 9.8 Hz, 1H), 3.38 (s, 3H), 2.96-2.94 (m, 3H), 2.50 (s, 6H), 1.43 (s, 6H). <sup>13</sup>C NMR:  $\delta$  155.3, 142.8, 141.2, 134.9, 132.2, 130.8, 128.3, 123.4, 121.1, 97.3, 86.9, 84.9, 80.8, 80.2, 80.0, 79.7, 79.5, 76.4, 74.9, 74.8, 74.6, 69.5, 68.5, 59.4, 59.2, 57.9, 57.8, 54.2, 13.6. Anal. Calcd for C<sub>38</sub>H<sub>39</sub>BF<sub>2</sub>N<sub>2</sub>O<sub>6</sub> (668.5): C, 68.27; H, 5.88; O, 14.36. Found: C, 67.59; H, 5.47; O, 14.74.





## Compound 2



[Pd(PPh<sub>3</sub>)<sub>4</sub>] (0.038 mmol) was added to a degassed solution of boron difluoro-2-[(3,5-dimethyl-2*H*-pyrrole-2-ylidene)-(4-iodophenyl)methyl]-3,5-dimethyl-1*H*-pyrrolate (**4**) (0.175 g, 0.38 mmol) and compound **7** (100 mg, 0.11 mmol) in DMF/TEA (14 ml, 1:1). The mixture was then heated, at 60°C, under argon, for 3 h, until the disappearance of compound **7** was observed by TLC (Hexane/EtOAc 1:1). Solvents were removed under reduced pressure. The reaction crude was subjected to silica gel column chromatography with Toluene/EtOAc (from Toluene 100% up to 95:5) for obtaining compound **2** as a deep green solid (0.13 g, 0.071 mmol, 65 %). TLC: *R<sub>f</sub>* 0.58 (eluant Toluene/EtOAc 95:5). Decomposition is observed from 95°C. <sup>1</sup>H NMR: δ 7.76-7.69 (m, 8H), 7.55-7.16 (m, 16H), 6.83-6.77 ((m, 6H), 6.08-6.06 (m, 6H), 5.05 (d, *J* = 3.4 Hz, 1H), 4.93-4.83 (m, 4H), 4.70 (s, 2H), 4.55 and 4.50 (AB system, *J* = 16.1 Hz, 2H), 4.04-3.98 (m, 3H), 3.81-3.76 (m, 2H), 3.71 (dd, *J* = 8.3 *J* = 9.8 Hz, 1H), 3.44 (s, 3H), 3.05 (s, 12H), 2.47 (s, 18H), 1.46 (s, 6H), 1.39 (s, 6H), 1.38 (s, 6H), 1.35 (s, 6H). <sup>13</sup>C NMR: δ 155.3, 152.8, 151.2, 142.7, 140.9, 140.5, 136.7, 135.6, 134.9, 134.8, 132.3, 132.2, 132.0, 130.8, 129.2, 128.7, 128.6, 128.3, 128.3, 127.9, 127.8, 126.3,



125.0, 124.5, 123.6, 123.5, 123.5, 123.1, 122.6, 121.1, 117.2, 114.0, 112.0, 97.3, 87.6, 87.4, 87.0, 86.9, 85.2, 85.1, 84.9, 84.8, 80.9, 79.6, 76.4, 69.8, 68.7, 60.2, 59.9, 58.6, 58.0, 57.9, 54.3, 39.2, 13.9, 13.7, 13.6, 13.5. Anal. Calcd for  $C_{113}H_{108}B_4F_8N_{10}O_6$  (1897,3): C, 71.53; H, 5.74; O, 5.06. Found: C, 70.67; H, 6.32; O, 5.58.

**Absorption and luminescence spectra of 6 and 7.**

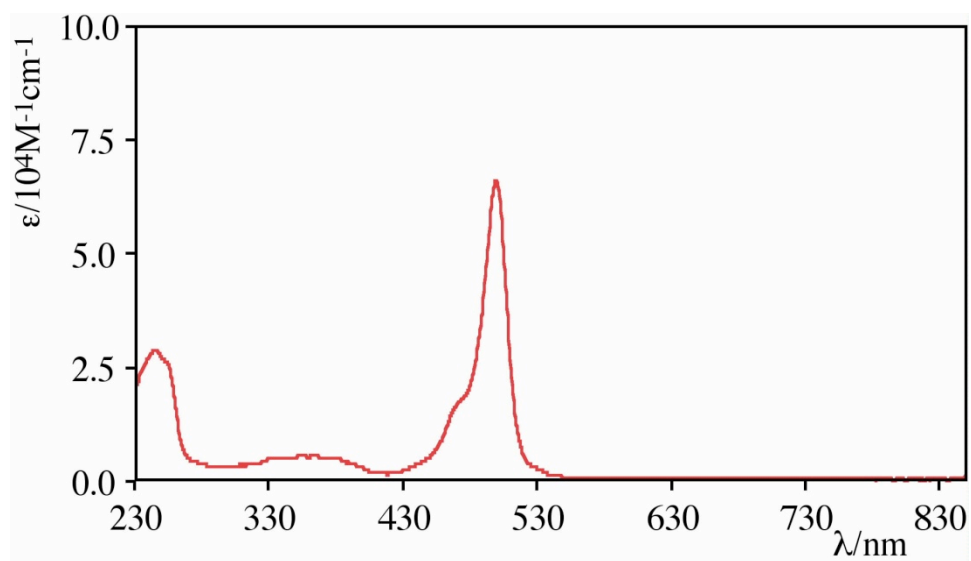


**Figure S.1.** Absorption spectrum of **6** in acetonitrile solution.

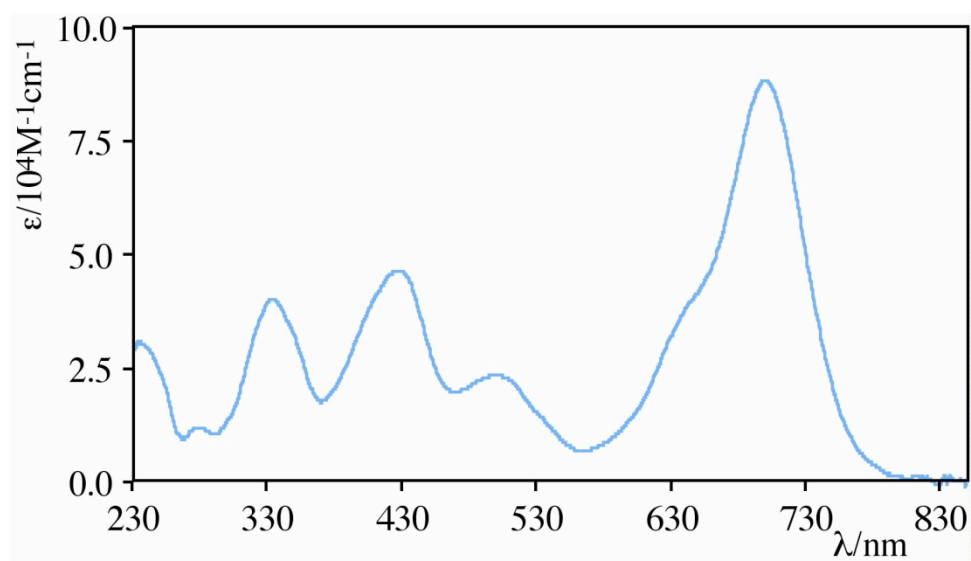


**Figure S.2.** Absorption spectrum of **7** in acetonitrile solution.

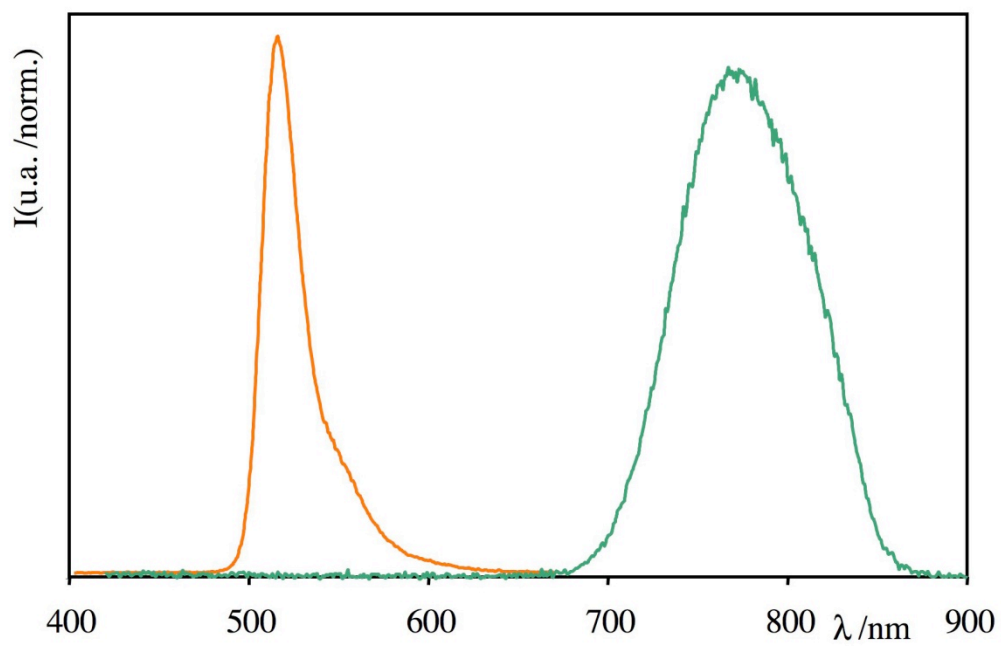
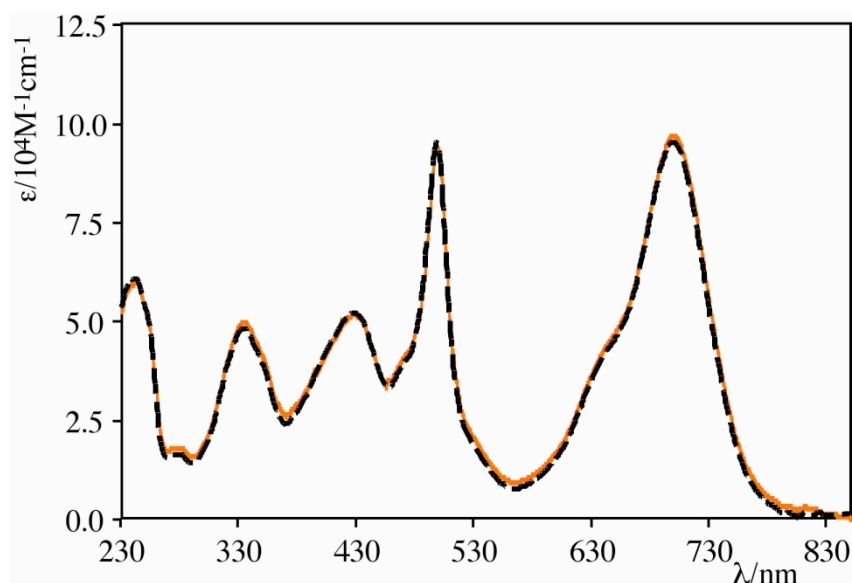


**Figure S.3.** Emission spectra of **6** (orange line) and **7** (green line) in acetonitrile solution at room temperature.

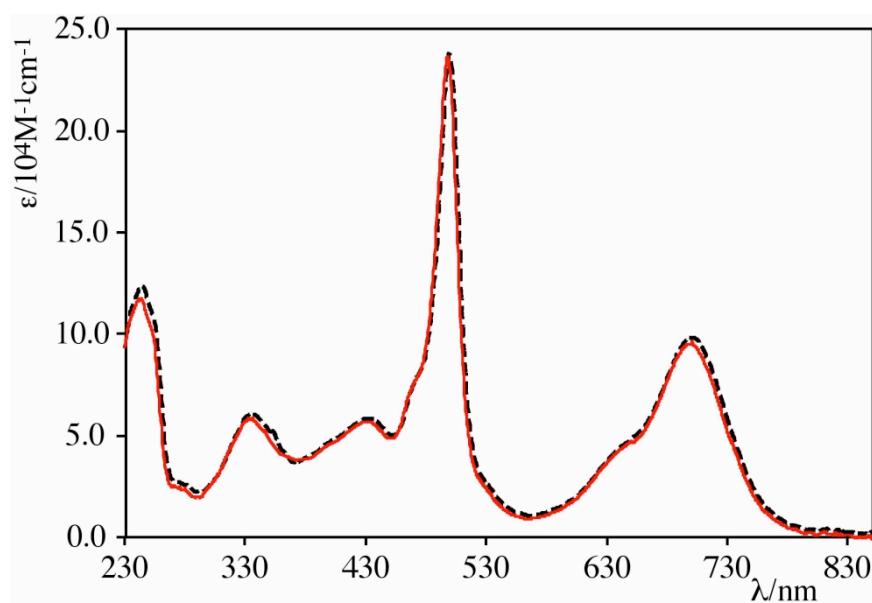
### Calculated sum spectra of 6 (one- or three-fold) plus 7 *versus* absorption spectra of 1 and 2.

Figure S4 shows the absorption spectrum of **1** and the curve obtained by adding the absorption spectrum of **6** to the spectrum of **7**, whereas Figure S5 reports the absorption spectrum of **2** and the curve obtained by adding three fold the spectrum of **6** to the spectrum of **7**.

The absorption spectra of **1** and **2** are essentially additive so indicating that each chromophoric subunit keeps its own spectroscopic properties in the multicomponent systems.



**Figure S.4.** Experimental absorption spectrum of **1** (black dashed line) versus the calculated curve (orange line) obtained by adding the absorption spectrum of **6** to the absorption spectrum of **7**.



**Figure S.5.** Experimental absorption spectrum of **2** (black dashed line) versus the calculated curve (orange line) obtained by adding three fold the absorption spectrum of **6** to the absorption spectrum of **7**.

### Excitation spectra of **1** and **2**.

Figures S.6 and S.7 show the excitation spectra of **1** and **2**, respectively, recorded for diluted solution (see overlaid curves) at 770 nm (emission energy maximum in both cases).

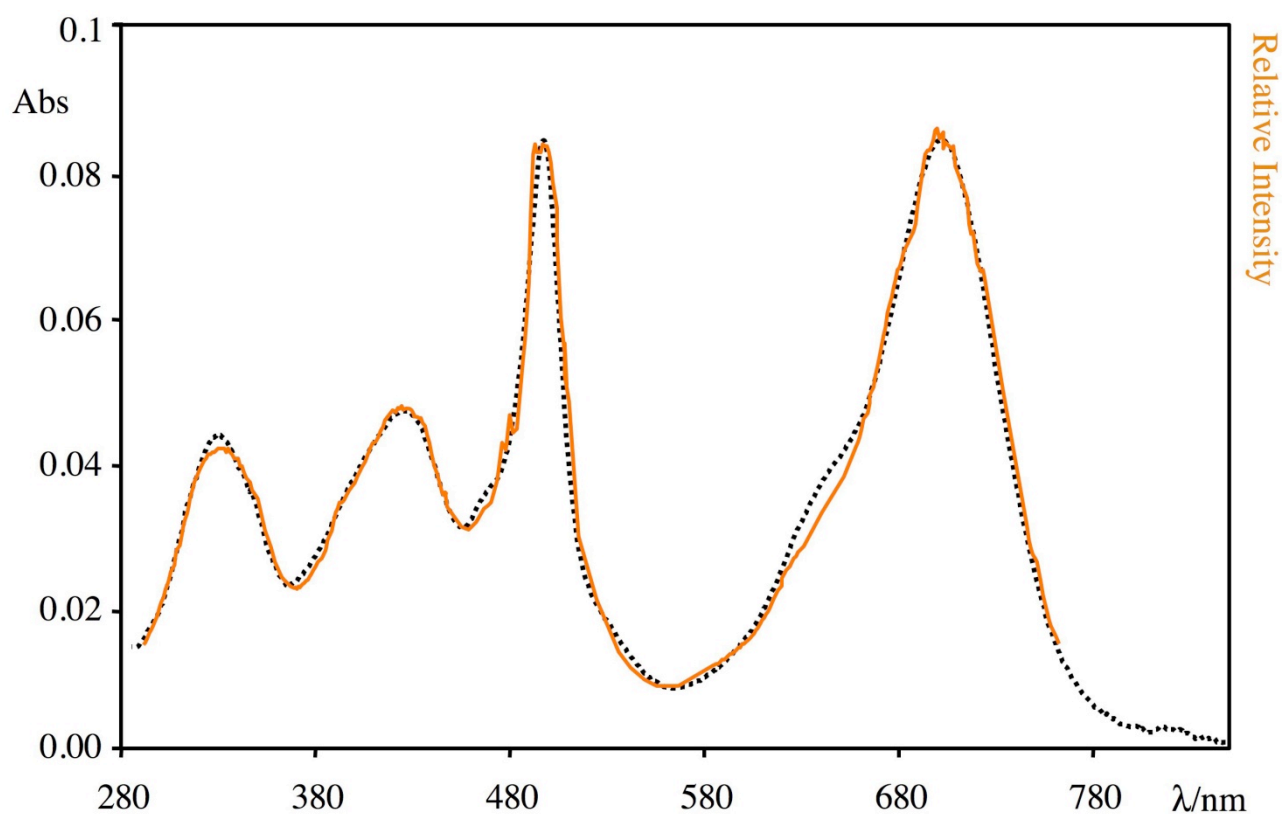


**Figure S.6.** Corrected excitation spectrum of **1** (in acetonitrile - orange line), recorded at the **B** emission energy maximum ( $\lambda = 770$  nm). The absorption spectrum of **1** is also reported (dotted curve).

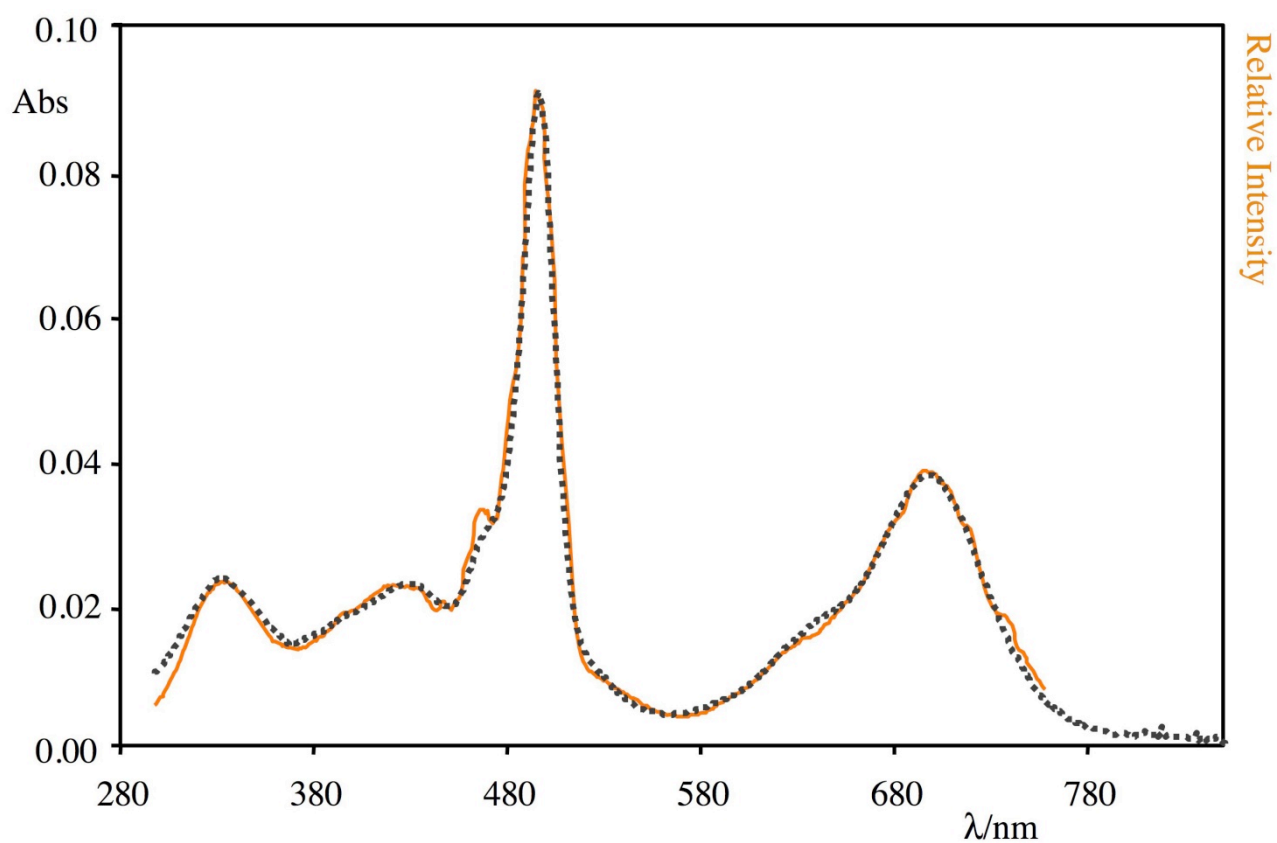


**Figure S.7.** Corrected excitation spectrum of **2** (in acetonitrile - orange line), recorded at the **B** emission energy maximum (770 nm). The absorption spectrum of **2** is also reported (dotted curve).

**Emission spectra of solution mixtures (1:1 and 3:1 molar ratio) of 6 and 7 in comparison with emission spectra of 1 and 2 (isoabsorbing solutions at the excitation wavelength, 360 nm)**

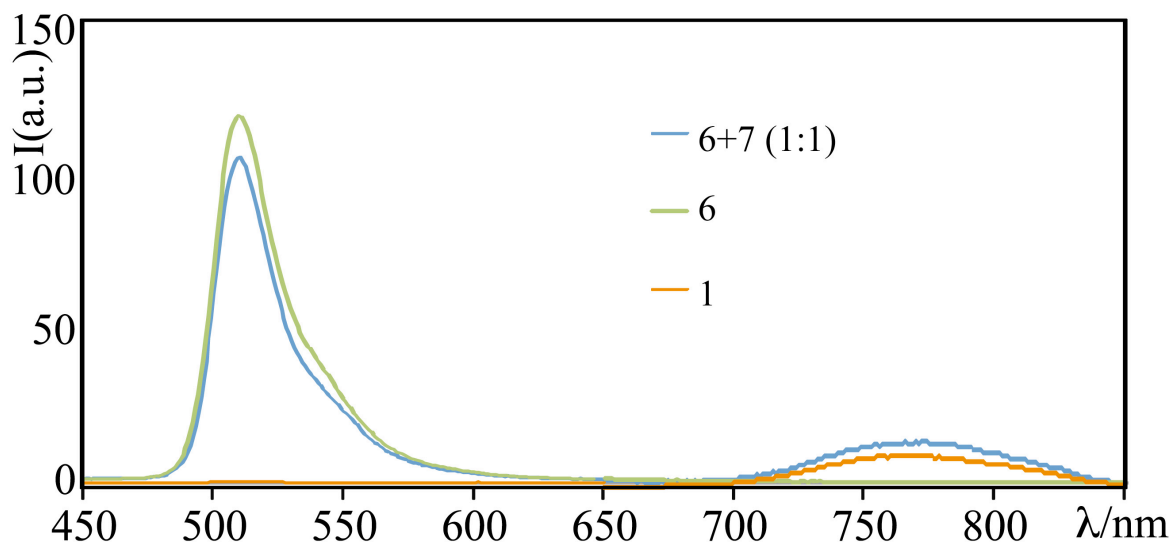


**Figure S.8.** Emission spectrum of a solution mixture of **6** and **7** in the molar ratio 1:1, in comparison with the emission spectra of **1** and **6** (isoabsorbing solutions at 360 nm - excitation wavelength).

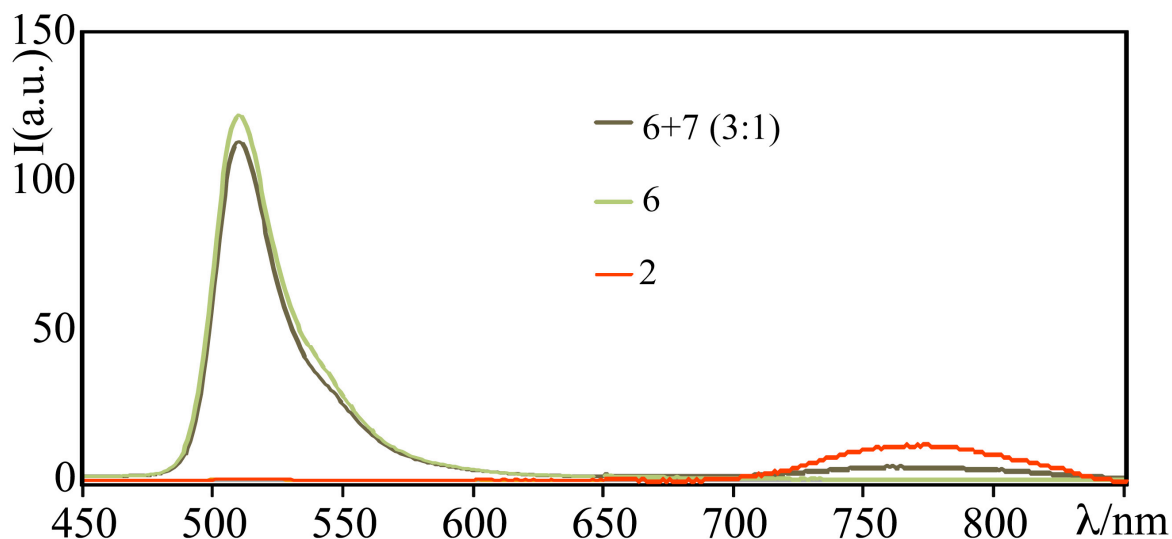


**Figure S.9.** Emission spectrum of a solution mixture of **6** and **7** in the molar ratio 1:1, in comparison with the emission spectra of **2** and **6** (isoabsorbing solutions at 360 nm - excitation wavelength).

## Transient absorption spectra of 6 and 7

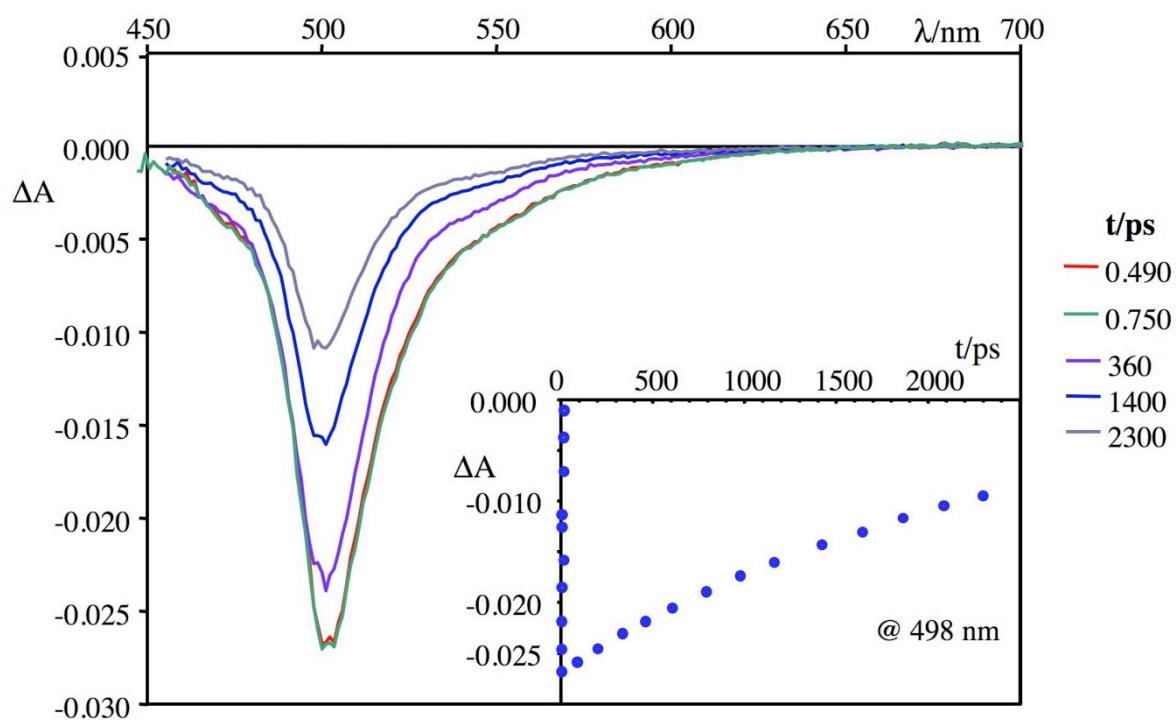


**Figure S.10.** Transient absorption spectra of **6** at different time delays after pump pulse (excitation wavelength: 400 nm, 2  $\mu$ J), in acetonitrile solution. The overall time decay at 498 nm is reported in the inset.



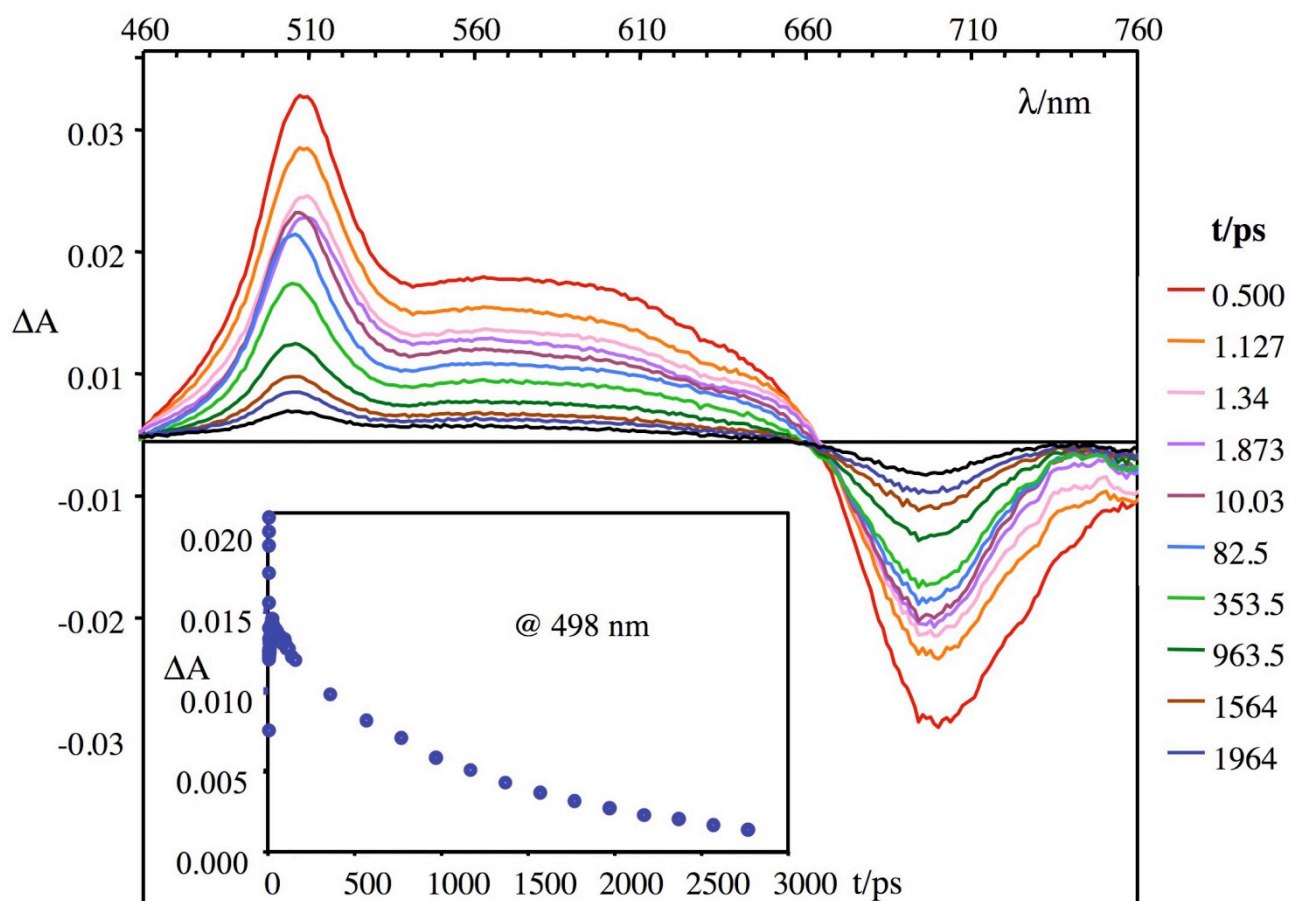


**Figure S.11.** Transient absorption spectra of 7 at different time delays after pump pulse (excitation wavelength: 400 nm, 2  $\mu\text{J}$ ), in acetonitrile solution. The overall time decay at 498 nm is reported in the inset.

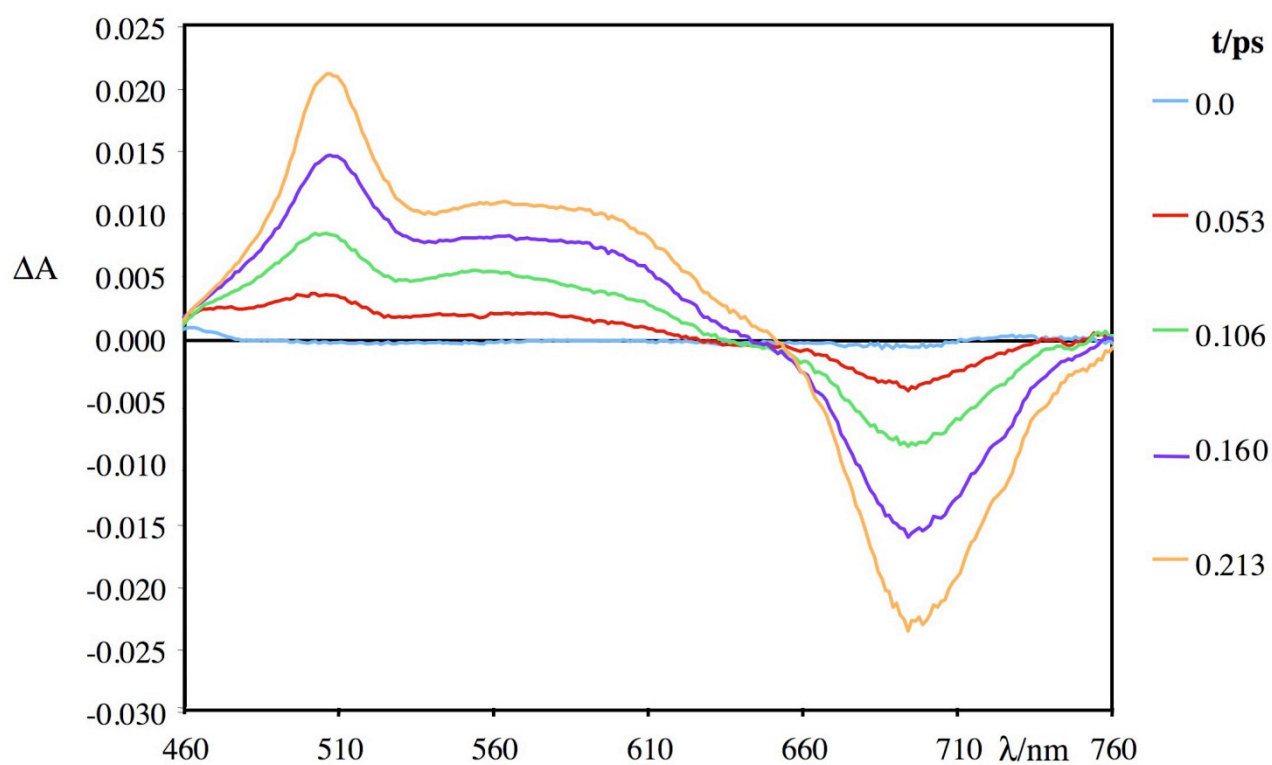


**Figure S.12.** Transient absorption spectra of **7** during the pump pulse, in acetonitrile solution. The present figure is reported to highlight the absence of a particular bleaching features at around 500 nm during the pump pulse in **7** with respect to transient spectra of **1** in the same time range (see main text).

---

## References

<sup>1</sup> Demas, J. N.; Crosby, G. A. *J. Phys. Chem.*, 1971, 75, 991

<sup>2</sup> Nakamaru, N. *Bull. Chem. Soc. Jpn.*, 1982, 55, 2697

<sup>3</sup> Magde, D.; Brannon, J. H.; Cremers, T. L.; Olmsted, J. *J. Phys. Chem.* 1979, 83, 2581.

<sup>4</sup> Ulrich, G.; Goeb, S.; De Nicola, A.; Retailleau, P. ; Ziessel, R. *Synlett* 2007, 1517.

<sup>5</sup> Förster, T. *Discuss Faraday Soc.* **1959**, 27, 7.

<sup>6</sup> F. Perez-Balderas, J. Morales-Sanfrutos, F. Hernandez-Mateo, J. Isaac-García, and F. Santoyo-Gonzales, *Eur. J. Org. Chem.*, 2009, 2441.

